ChemEngineering

MDPI

Article

Biodiesel Carbonaceous Nanoparticle-Supported Potassium Carbonate as a Catalyst for Biodiesel Production via Transesterification

Chuan Li [1,2,3], Tianyu Shi [2], Yijun Chen [3], Li Zhang [3], Zhiquan Yang [4], Lin Xu [5], Yong Luo [1,*] and Xiaoyong Xu [2,*]

[1] School of Chemical Engineering & Technology, China University of Mining and Technology, Xuzhou 221116, China; 053039@chu.edu.cn
[2] School of Chemistry and Material Engineering, Chaohu University, Hefei 238000, China; shi006126@163.com
[3] Huangshan Shangyi Rubber and Plastic Products Co., Ltd., Huangshan 245500, China; chenyj94@126.com (Y.C.); hssy666@sohu.com (L.Z.)
[4] School of Mechanical Engineering, Chaohu University, Hefei 238000, China; yzq1614221751@163.com
[5] Pingxiang Best Insulator Group Co., Ltd., Pingxiang 337000, China; tangh_19@163.com
* Correspondence: sulyflying@cumt.edu.cn (Y.L.); xxy1310@163.com (X.X.)

Abstract

This study primarily focuses on the development and optimization of a high-efficiency catalyst for biodiesel production. Potassium carbonate-supported solid catalysts were synthesized using soot as the support material via an equal-volume impregnation method. Transmission electron microscopy (TEM) and X-ray diffraction (XRD) analyses confirmed the successful deposition of potassium carbonate onto the soot surface, resulting in uniformly dispersed spherical nanoparticles on the catalyst. The catalytic performance was evaluated through single-factor experiments, assessing the effects of catalyst loading, alcohol-to-oil molar ratio, reaction temperature, and reaction time on the transesterification reaction. The maximum biodiesel yield obtained from the Single-factor experiments was 95.29% under the optimal conditions of 6 wt% catalyst loading (relative to oil), alcohol-to-oil molar ratio of 14:1, reaction temperature of 60 °C, and reaction time of 3 h. Furthermore, response surface methodology (RSM) using a four-factor, three-level Box–Behnken design (BBD) was employed to systematically analyze the interaction effects of these variables on the biodiesel yield. The optimized conditions identified by RSM were 61.1 °C, 3.3 h, alcohol-to-oil molar ratio of 14.2:1, and 6.1 wt% catalyst dosage, yielding 95.37% biodiesel conversion. These findings demonstrate that the soot-supported potassium carbonate catalyst developed in this study exhibits excellent catalytic activity, offering a novel catalyst system for industrial biodiesel production with significant academic and practical potential.

Keywords: biodiesel; catalyst; transesterification reaction; soot

check for updates

Academic Editor: Venko N. Beschkov

Received: 7 August 2025
Revised: 16 September 2025
Accepted: 17 October 2025
Published: 22 October 2025

Citation: Li, C.; Shi, T.; Chen, Y.; Zhang, L.; Yang, Z.; Xu, L.; Luo, Y.; Xu, X. Biodiesel Carbonaceous Nanoparticle-Supported Potassium Carbonate as a Catalyst for Biodiesel Production via Transesterification. *ChemEngineering* **2025**, *9*, 116. https://doi.org/10.3390/chemengineering9060116

Copyright: © 2025 by the authors. Licensee MDPI, Basel, Switzerland. This article is an open access article distributed under the terms and conditions of the Creative Commons Attribution (CC BY) license (https://creativecommons.org/licenses/by/4.0/).

1. Introduction

Biodiesel is an environmentally friendly biofuel primarily produced through the transesterification of animal fats, vegetable fats, or waste cooking oil with short-chain alcohols (such as methanol or ethanol) in the presence of a catalyst. The major product, fatty acid methyl ester (FAME), exhibits physicochemical properties that closely resemble those of conventional petroleum-based diesel fuel and, in some respects, even surpass it in specific performance metrics [1]. From an environmental standpoint, biodiesel offers significant advantages, notably its ability to substantially reduce particulate matter (PM) emissions.

Even under high-load engine conditions, PM emissions from biodiesel remain consistently lower than those from traditional diesel fuels [2,3]. As a renewable, biodegradable, and low-emission alternative, biodiesel holds great potential for addressing global energy and environmental challenges [4]. It has been demonstrated to effectively reduce greenhouse gas emissions and mitigate environmental pollution [5]. Moreover, biodiesel production enables the conversion of plant oils, microalgae, and waste biomass into a liquid fuel that is highly compatible with existing diesel engines, providing a direct solution to energy security issues while significantly reducing emissions of sulfur oxides, particulate matter, and greenhouse gases [6,7]. Thus, biodiesel functions as a vital component of renewable energy strategies.

Currently, biodiesel is primarily synthesized via transesterification, wherein triglycerides react with methanol in the presence of acid or base catalysts to produce fatty acid methyl esters. Alkaline catalysts are widely employed in both industrial and laboratory settings due to their high catalytic activity and low cost. For instance, Chanakaewsomboon et al. [8] utilized potassium methoxide as a homogeneous catalyst for the transesterification of refined palm oil, achieving high activity and selectivity owing to its uniform dispersion and effective interaction with reactants. Similarly, Golmakani et al. [9] reported a conversion rate exceeding 95% using potassium hydroxide combined with microwave-assisted heating for the transesterification of sour cherry kernel oil, with yields increasing alongside catalyst concentration. However, traditional homogeneous alkaline catalysts have several drawbacks, such as difficulties in product separation and equipment corrosion. In contrast, solid catalysts offer advantages including ease of recovery, reusability, and environmental compatibility, making them an increasingly attractive alternative. Olagunju et al. [10] utilized a CaO/activated-carbon composite catalyst in a membrane reactor to continuously convert soybean oil into biodiesel, achieving a conversion rate of 96.9% under optimal conditions, with the resulting fuel meeting quality standards. Cong et al. [11] synthesized a solid base catalyst from waste bleaching clay ash and achieved a biodiesel yield exceeding 90% at 65 °C. These studies demonstrate that solid alkali catalysts not only provide high conversion efficiency but also offer recyclability and environmental benefits, making them a promising solution for future biodiesel production [12,13].

The abundant surface functional groups and high chemical stability of soot make it an appealing support material for catalysts. For example, Singh et al. [14] developed a cost-effective and efficient fuel cell electrode using soot, demonstrating its potential as a convenient, high-performance, and low-cost catalyst support. In addition to these properties, soot offers a high surface area, chemical stability, and good electrical conductivity, which enhance catalyst dispersion and stability during transesterification.

Single-factor experimental methods remain a reliable approach for elucidating the influence of individual variables in biodiesel production. This method enables a clear assessment of each parameter's effect on yield, providing a scientific foundation for process optimization. Xiang et al. [15] applied this approach to determine the optimal particle size, reaction pressure, temperature, and the methanol-to-oil ratio for biodiesel synthesis, achieving a yield of 96.21% under conditions of 60 mesh particle size, 16 MPa pressure, 100 °C temperature, a reaction time of 180 min, and a molar ratio of 35:1. Baig and Ng [16] studied the effect of catalyst dosage, alcohol-to-oil ratio, and free fatty acid content, achieving a 93.95% yield from soybean oil containing 10% palmitic acid under optimal conditions: a reaction temperature of 200 °C, an alcohol-to-oil molar ratio of 27:1, and a catalyst dosage of 3 wt%. Chen et al. [17] used KF/CaO as a solid base catalyst supported by ultrasonication to catalyze the transesterification of soybean oil with methanol, identifying optimal conditions through single-factor analysis. These studies validate the effectiveness

of single-variable optimization in identifying key factors that influence biodiesel production, facilitating the establishment of efficient and cost-effective production processes.

Response surface methodology (RSM) offers a systematic and statistically rigorous framework for process optimization, grounded in mathematical statistics and experimental design. Quantitative modeling elucidates the relationships between multiple factors and their responses. RSM is widely applied in fields such as food processing, biotechnology, and chemical engineering [18–20], demonstrating considerable value. This method offers clear advantages over traditional experimental approaches, such as single-factor and orthogonal experimental designs: it significantly reduces the experimental workload by decreasing the number of experiments by 50–70%, thereby conserving resources. Additionally, RSM captures second-order nonlinear interactions among variables, enabling accurate characterization of response behavior in complex models. It also facilitates quantitative analysis of multi-dimensional interactions.

This study aims to address the challenges associated with conventional homogeneous alkaline catalysts, including product separation difficulties, yield contamination, and catalyst deactivation, by employing soot as a novel support for potassium carbonate. An equal-volume impregnation method was employed to achieve uniform dispersion of the active component on the carbon carrier. Single-factor experiments were conducted to evaluate the effects of the alcohol-to-oil molar ratio, catalyst dosage, reaction time, and temperature on biodiesel yield. Each experiment was performed in triplicate, and average values were reported to ensure reproducibility. Subsequently, RSM was employed to optimize the reaction conditions, ultimately establishing a high-performance catalyst system for biodiesel production.

2. Materials and Methods

The primary materials used in this study include Biodiesel Carbonaceous Nanoparticles (BCNs), also known as biodiesel soot, which were collected using a custom-built soot collection apparatus. Potassium carbonate (K_2CO_3, analytical grade) was used for catalyst preparation. Additional materials included cottonseed oil (used as the feedstock for the transesterification reaction, with an acid value of 0.52 mg KOH/g and a moisture content below 0.1%.), methanol (chemical grade), deionized water (used to prepare K_2CO_3 solutions), and color-indicating silica gel (used to store catalysts in a dry environment to prevent moisture-induced deactivation).

2.1. Catalyst Preparation

BCN was initially ground and then dried in an oven at 110 °C for 2 h. After drying, the BCN was stored in a desiccator containing silica gel to prevent moisture absorption. The catalyst was prepared using an equal-volume impregnation method. Specifically, 5 g of K_2CO_3 was dissolved in 50 mL of deionized water, and 10 g of BCN was gradually added under continuous stirring. The volume of the solution was carefully controlled to just cover the surface of the BCN. The mixture was stirred for 2 h and subsequently allowed to stand for 24 h to facilitate impregnation. Subsequently, the sample was subjected to evaporation at 80 °C to remove residual moisture, followed by oven drying at 120 °C for 10 h. After drying, the solid was ground into a fine powder once the temperature fell below 80 °C and stored in a sealed desiccator with silica gel to maintain dryness and prevent deactivation for further usage.

The 50 wt% K_2CO_3 loading was selected based on preliminary optimization experiments conducted in this study, as well as guidance from the literature [21]. It is important to note that soot composition can vary depending on the combustion source; therefore, a standardized collection method was employed to ensure reproducibility [22,23].

2.2. Characterizations

X-ray diffraction (XRD) was employed to analyze phase changes during catalyst preparation (Rigaku D/MAX-2500, Tokyo, Japan). Field Emission Scanning Electron Microscopy (FESEM) (Hitachi S-4800, Tokyo, Japan) was used to examine the surface morphology and particle size distribution. Field Emission Transmission Electron Microscopy (FETEM) (JEOL JEM-2100F, Tokyo, Japan) provided detailed observations of the catalyst's nanoscale structure and morphology. Elemental composition was analyzed using Energy-Dispersive X-ray Spectroscopy (EDS) (Oxford Instruments, Oxford, UK). The preparation of biodiesel by transesterification reaction was carried out in a 250 mL 3-necked flask, and the reaction was controlled by heating in a water bath under magnetic stirring conditions temperature. First, mix 30 g of cotton seed oil, a certain proportion of anhydrous methanol, and catalyst. Place the chemical agent in a round bottom flask. Heat the mixture under magnetic stirring. At a certain temperature, condense and reflux. After a certain reaction time, centrifuge and separate. Separate the catalyst and the liquid phase product into layers using a separatory funnel, with glycerol as the lower layer. The upper layer is a crude product. The biodiesel yield was calculated indirectly by measuring the conversion of glycerol, which reflects the biodiesel conversion, as described in the referenced study [24].

2.3. Response Surface Methodology (RSM)

Response surface methodology (RSM) was employed using a Box–Behnken Design (BBD) to analyze the interaction effects of four factors: reaction temperature (55–65 °C), reaction time (2–4 h), alcohol-to-oil molar ratio (12:1–16:1), and catalyst dosage (5–7 wt%). A total of 29 experiments were conducted, and a quadratic polynomial regression model was developed to predict biodiesel yield. Statistical analysis was performed using Design-Expert software (Version 12).

3. Results and Discussion

3.1. Catalysts Characterization

Figure 1 presents the SEM images of BCN, the K_2CO_3/BCN catalyst precursor, and the K_2CO_3/BCN catalyst. As shown in Figure 1a, the pristine BCN exhibits a block-like morphology, attributed to particle agglomeration. Figure 1b shows that after impregnation and drying, the catalyst precursor retains a similar morphology, indicating that agglomeration persists during the early stages of catalyst preparation. Following calcination (Figure 1c), K_2CO_3 particles are visibly loaded and sintered onto the surface of the BCN, forming a compact, agglomerated structure. Although potassium carbonate can act as a catalyst, it dissolves in the reaction mixture, making it unsuitable for reuse. BCN is a carbon-based material that serves effectively as a catalyst support but is not an efficient catalyst for transesterification reactions. Overall, the surface morphology of the K_2CO_3/BCN catalyst demonstrates a block-like agglomerated configuration.

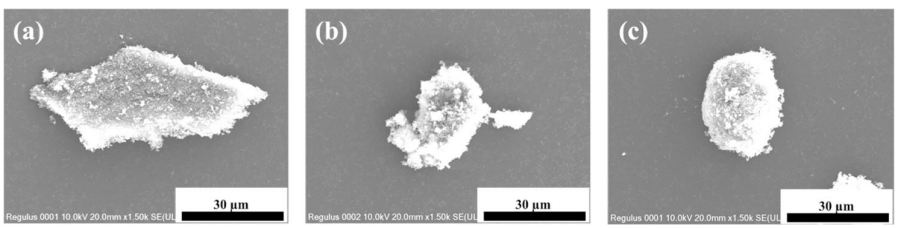


Figure 1. SEM images of (**a**) BCN, (**b**) K_2CO_3/BCN catalyst precursor, and (**c**) K_2CO_3/BCN catalyst.

TEM analysis further illustrates the structure of BCN and K_2CO_3/BCN catalysts. Figure 2a,b show that BCN consists of uniformly spherical particles connected in a chain-

like arrangement, likely due to van der Waals forces. Similarly, Figure 2c,d demonstrate that the K_2CO_3/BCN catalyst maintains a spherical morphology, with the particles still exhibiting chain-like connectivity. Both SEM and TEM images confirm that K_2CO_3 particles are well dispersed without altering the spherical morphology of BCN. Literature reports indicate that soot-supported catalysts typically benefit from a relatively high surface area, which facilitates reactant accessibility and dispersion of active sites [24].

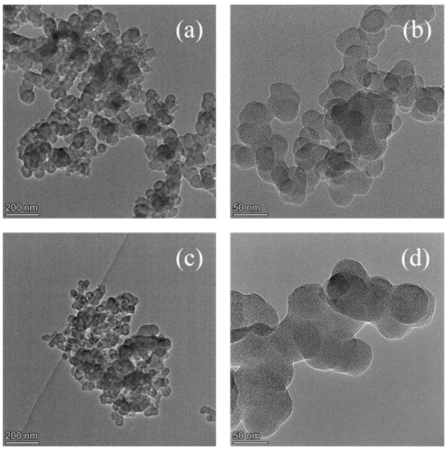


Figure 2. TEM images of (**a**,**b**) BCN and (**c**,**d**) K_2CO_3/BCN catalyst.

EDS was employed to determine the elemental composition and distribution within the catalyst (Figure 3). The analysis confirmed the presence of C, O, and K. C and O originate from the BCN support and K_2CO_3, while K primarily derives from K_2CO_3. The uniform distribution of potassium across the surface indicates successful and homogeneous loading of K_2CO_3 onto the BCN matrix. In addition, approximate mass fraction was determined: C ≈ 87.6 wt%, O ≈ 9.5 wt%, and K ≈ 2.9 wt%.

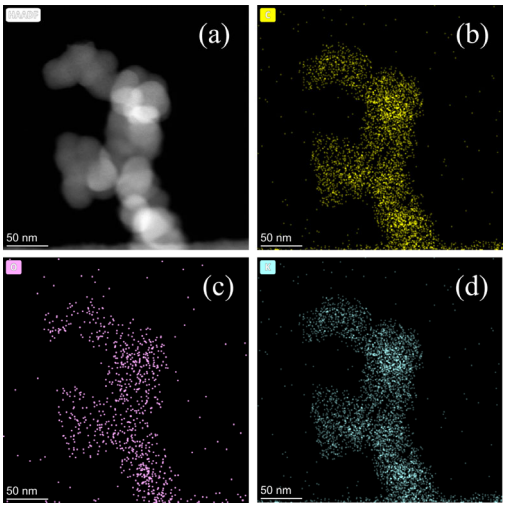


Figure 3. EDS mapping of (**a**) the K_2CO_3/BCN catalyst; (**b**) C element; (**c**) O element; and (**d**) K element.

XRD patterns of the BCN support, catalyst precursor, and final catalyst are presented in Figure 4. The BCN exhibits characteristic graphite diffraction peaks at 2θ = 24.4° and 44.1°, confirming the presence of a graphite-like structure [25]. The K_2CO_3/BCN precursor exhibits additional diffraction peaks at 2θ = 30.2°, 31.6°, 38.1°, and 40.9°, corresponding to K_2CO_3, indicating successful impregnation. After calcination, the K_2CO_3/BCN catalyst exhibits a new diffraction peak at 2θ = 29.2°, corresponding to K_2O. This suggests that partial thermal decomposition of K_2CO_3 to K_2O occurred during catalyst preparation.

Therefore, the active species in the final K_2CO_3/BCN catalyst include both K_2CO_3 and K_2O, confirming the formation of a typical supported solid base catalyst [26].

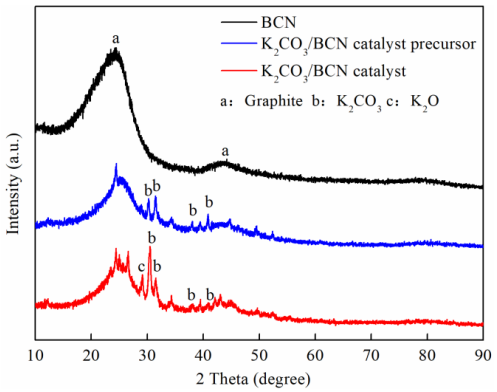


Figure 4. XRD patterns of (a) BCN, (b) K_2CO_3/BCN catalyst precursor, and (c) K_2CO_3/BCN catalyst.

3.2. Single-Factor Experiments

Figure 5 illustrates the effect of reaction time on biodiesel yield under fixed conditions: an alcohol-to-oil molar ratio of 12:1, a catalyst dosage of 3 wt%, and a reaction temperature of 60 °C. Biodiesel yield increased progressively with reaction time, reaching a maximum after 3 h. Prolonging the reaction time beyond this point resulted in a slight decrease in yield, likely due to side reactions such as emulsification. Consequently, 3 h was identified as the optimal reaction time for the transesterification process [27]. Although the difference in yield between 2 h and 3 h was relatively small, 3 h was selected to ensure maximum conversion and reproducibility.

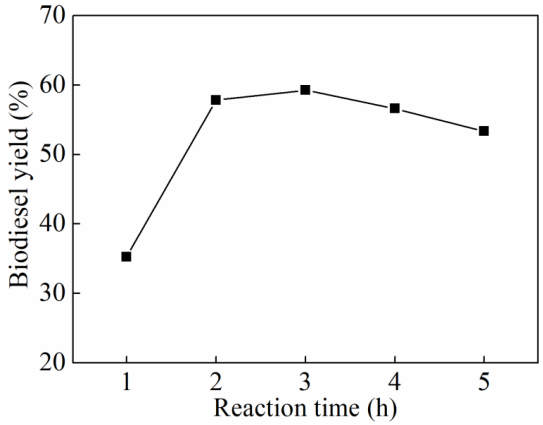


Figure 5. Effect of reaction time on biodiesel yield.

As depicted in Figure 6, the catalyst dosage varied while maintaining constant reaction conditions: 3 h of reaction time, 60 °C reaction temperature, and an alcohol-to-oil molar ratio of 12:1. The biodiesel yield increased from 59.28% to 85.63% as the catalyst loading rose from 3 wt% to 6 wt%. However, further increases in catalyst dosage resulted in a decline in yield. This decrease can be attributed to agglomeration of catalyst particles and the occurrence of side soap-formation reactions at higher catalyst loadings. Based on this analysis, a catalyst dosage of 6 wt% was determined to be optimal [28].

Figure 7 illustrates the effect of the methanol dosage (alcohol-to-oil molar ratio) on biodiesel yield, with fixed parameters: a reaction time of 3 h, a temperature of 60 °C, and a catalyst loading of 6 wt%. Increasing the methanol-to-oil ratio from 10:1 to 14:1 resulted in a gradual improvement in biodiesel yield. However, further increasing the ratio to 18:1 caused a decrease in yield. Therefore, a molar ratio of 14:1 was determined to provide the highest conversion efficiency [29].

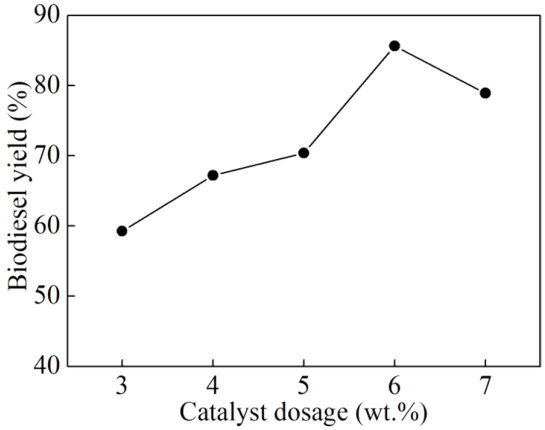


Figure 6. Effect of catalyst dosage on biodiesel yield.

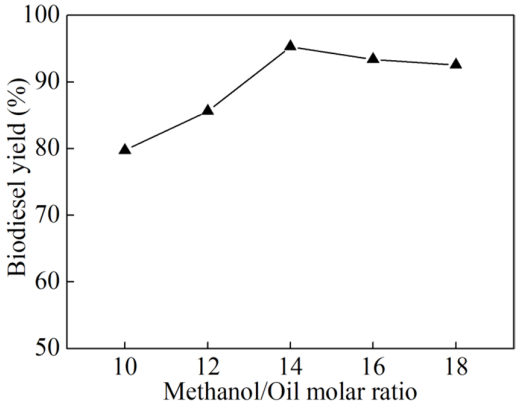


Figure 7. Effect of alcohol-to-oil molar ratio on biodiesel yield.

Figure 8 shows the effect of reaction temperature on biodiesel yield under fixed conditions: a reaction time of 3 h, an alcohol-to-oil molar ratio of 14:1, and a catalyst dosage of 6 wt%. The yield increased as the temperature rose from 50 °C to 60 °C, reaching a maximum at 60 °C. Beyond this temperature, the yield declined, likely due to methanol volatilization and the further hydrolysis of higher fatty acid methyl esters into free fatty acids caused by the elevated temperature, which reduces biodiesel yield. Therefore, 60 °C was identified as the optimal temperature for the transesterification process and biodiesel production [30].

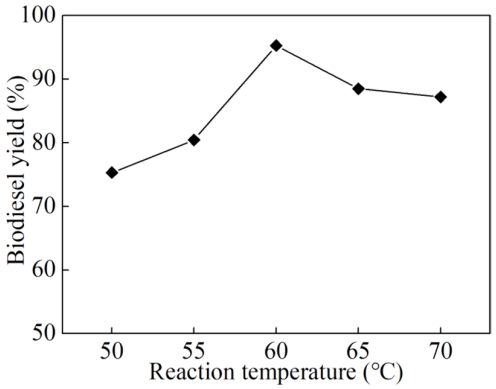


Figure 8. Effect of reaction temperature on biodiesel yield.

The reaction mechanism can be described as follows: the K_2CO_3/BCN catalyst provides strong basic sites that generate methoxide ions from methanol. These methoxide

ions then attack the carbonyl groups of triglycerides, leading to the formation of fatty acid methyl esters (biodiesel) and glycerol. Both K_2CO_3 and K_2O species present in the catalyst contribute to this catalytic pathway.

3.3. Response Surface Optimization Experiment

3.3.1. Box–Behnken Design (BBD) of Experiments

To investigate the key variables affecting oil-to-biodiesel conversion efficiency, a four-factor, three-level BBD was employed within a RSM optimization framework. A total of 29 experimental runs were conducted, as summarized in Table 1.

Table 1. Experimental design and results of the BBD.

Run	A (°C)	B (h)	C	D (wt%)	Yield (%)
1	55	3	14	7	65.81
2	60	4	12	6	75.42
3	60	3	14	6	95.12
4	65	2	14	6	90.08
5	60	3	14	6	95.19
6	60	2	14	7	83.35
7	55	2	14	6	80.45
8	55	3	12	6	69.16
9	60	4	14	5	65.53
10	60	3	14	6	95.13
11	65	3	14	5	60.52
12	55	3	14	5	74.16
13	60	3	14	6	95.03
14	60	2	14	5	82.3
15	60	4	16	6	92.61
16	60	3	12	7	81.63
17	60	3	16	7	89.3
18	60	4	14	7	92.01
19	60	2	12	6	91.78
20	65	3	16	6	92.64
21	65	4	14	6	84.05
22	60	3	12	5	66.79
23	60	3	14	6	94.89
24	60	2	16	6	93.15
25	65	3	12	6	82.39
26	65	3	14	7	92.55
27	60	3	16	5	82.65
28	55	4	14	6	78.16
29	55	3	16	6	83.12

3.3.2. Quadratic Model Analysis

Following the previous results, a second-order polynomial regression model was constructed utilizing Design Expert analysis:

$$Y = 95.07 + 4.28A - 2.78B + 5.53C + 6.06D - 9.63A^2 - 2.66B^2 - 3.69C^2 - 11.69D^2 - 0.9350AB - 0.9275AC + 10.09AD + 3.95BC + 6.36BD - 2.05CD \quad (1)$$

Analysis of variance (ANOVA) was used to evaluate the statistical significance of the model (see Table 2), where F and p are utilized to measure the visibility of the model and model projects. $p < 0.05$ indicates credible robustness and significant predictive effects on the response with a reliability of 95%. The model yielded an F-value of 80.13 and a p-value < 0.0001, indicating strong statistical reliability and excellent predictive performance.

However, the significant lack of fit ($p < 0.0001$) suggests that additional higher-order interactions not included in the quadratic model may exist. The model is nevertheless suitable for describing biodiesel yield trends within the studied factor ranges. Analysis of the experimental data confirmed that the quadratic polynomial regression model provides a satisfactory fit for the response surface, with the system behavior accurately captured within the specified range of independent variables. The results validate the model's effectiveness for predicting and optimizing biodiesel conversion rate.

Table 2. ANOVA for the response surface quadratic model.

Source	Sum of Squares	Degree of Freedom (Dom)	Mean Squares	*F*-Value	*p*-Value × Prob > *F*
Model	3037.26	14	216.95	80.13	<0.0001
A—Temperature	219.91	1	219.91	81.23	<0.0001
B—Time	92.57	1	92.57	34.19	<0.0001
C—Molar ratio	366.31	1	366.31	135.30	<0.0001
D—Catalyst addition	440.44	1	440.44	162.69	<0.0001
AB	3.50	1	3.50	1.29	0.2748
AC	3.44	1	3.44	1.27	0.2785
AD	407.64	1	407.64	150.57	<0.0001
BC	62.57	1	62.57	23.11	0.0003
BD	161.67	1	161.67	59.72	<0.0001
CD	16.77	1	16.77	6.19	0.0260
A^2	601.97	1	601.97	222.35	<0.0001
B^2	45.84	1	45.84	16.93	0.0011
C^2	88.31	1	88.31	32.62	<0.0001
D^2	887.14	1	887.14	327.69	<0.0001
Residual	37.90	14	2.71		
Lack of fit	37.85	10	3.78	277.88	<0.0001
Pure error	0.0545	4	0.0136		
Corr. total	3075.16	28			
$R^2 = 0.9877$					
R^2 Adj. = 0.9753					

3.4. Characterization Analysis of Response Surface Methodology

Figure 9 presents the three-dimensional response surface plots illustrating the interactions between various transesterification reaction parameters. Each surface plot captures the effect of two independent variables as well as the other two variables that are constant at their central values. These figures offer intuitive insights into the interaction effect under different conditions.

Figure 9a displays the interaction between reaction temperature and time, with the alcohol-to-oil molar ratio and catalyst dosage held constant at 14:1 and 6 wt%, respectively. The results indicate that when the temperature exceeds 60 °C, the oil conversion rate remains consistently above 83.35% through the transesterification, suggesting that reaction time exerts a relatively minor influence in this temperature range.

Figure 9b shows the interaction between reaction temperature and alcohol-to-oil molar ratio. An increase in temperature significantly enhances the oil conversion rate. Since the maximum yield was observed at 65 °C, a conversion rate of 82.39% can be achieved despite the alcohol-to-oil molar ratio. However, when the molar ratio exceeds 12:1, an oil conversion rate of ester content surpassing 90.0% can be achieved at a temperature of 65 °C.

Figure 9c examines the combined effects of reaction temperature and catalyst dosage, with reaction time and molar ratio fixed at 3 h and 12:1, respectively. The data demonstrate that both higher temperatures and increased catalyst loading substantially promote oil

conversion. When the amount of fixed the catalyst dosage was 7 wt%, the conversion rate increased from 65.43% to about 94.63% when the reaction temperature increased from 55 °C to 65 °C. Similarly, with a fixed reaction temperature of 65 °C and an increase in the catalyst dosage from 5 to 7, the conversion rate increased from 61.87% to 92.55%.

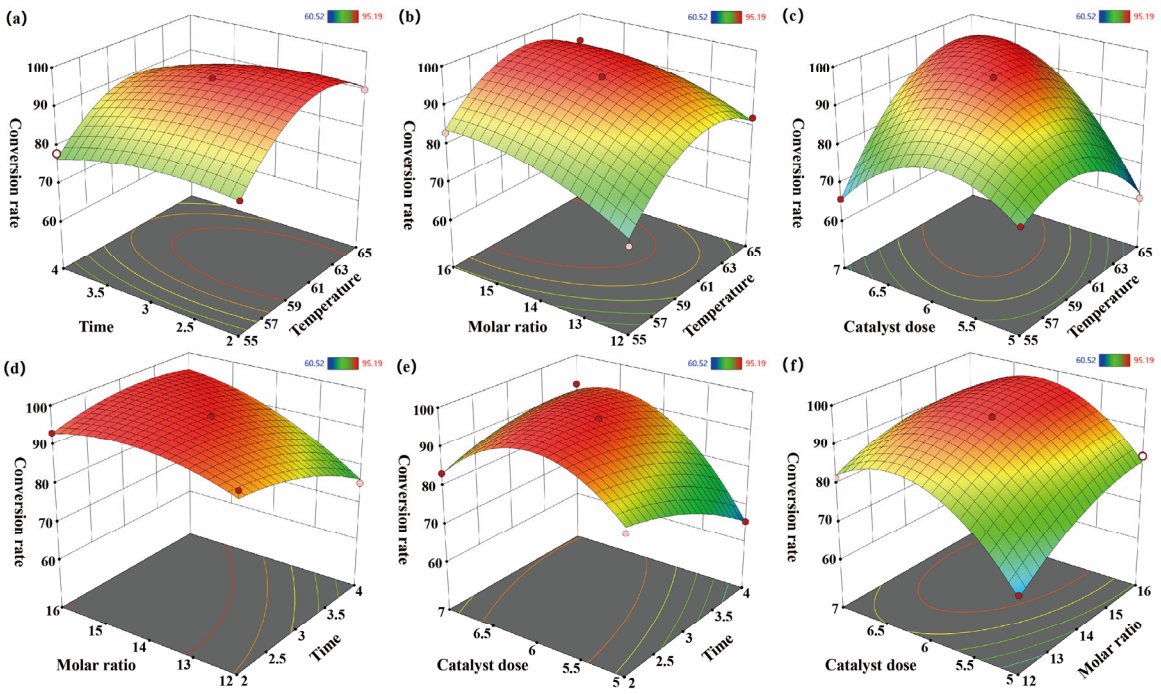


Figure 9. Three-dimensional response surface plots showing the effects of reaction parameters on biodiesel conversion rate: (**a**) reaction time and temperature; (**b**) methanol-to-oil molar ratio and temperature; (**c**) catalyst dosage and temperature; (**d**) methanol-to-oil molar ratio and reaction time; (**e**) catalyst dosage and reaction time; (**f**) catalyst dosage and methanol-to-oil molar ratio.

Figure 9d explores the interaction between reaction time and alcohol-to-oil molar ratio. The conversion rate consistently exceeds 89.0% across all tested molar ratios when reaction times are relatively short, reaffirming that reaction time has limited influence in this context. Figure 9e illustrates the interplay between reaction time and catalyst dosage. Catalyst loading has a strong positive effect on transesterification due to the increased availability of active sites. However, prolonged reaction times may reduce yield due to the reversible nature of the transesterification reactions.

Figure 9f reveals the interaction between the alcohol-to-oil molar ratio and catalyst dosage, indicating a significant influence. The contour lines along the catalyst axis are notably denser, indicating that catalyst concentration has a more pronounced effect on conversion than the molar ratio.

Based on the RSM predictions, the optimal reaction conditions were determined to be: 61.127 °C, 3.311 h, an alcohol-to-oil molar ratio of 14.199:1, and a catalyst dosage of 6.085 wt%, yielding a predicted oil conversion rate of 95.753%. For practical application, these values were rounded to 61.1 °C, 3.3 h, a molar ratio of 14.2:1, and a 6.1 wt% catalyst loading. Under these conditions, the experiment was repeated three times, producing conversion rates of 95.22%, 95.39%, and 95.43%, with an average of 95.37%. This outcome closely matches the model's prediction, confirming its reliability and accuracy in simulating the effects of various reaction parameters on oil conversion efficiency [31,32].

4. Conclusions

(1) The K_2CO_3/BCN catalyst exhibits a spherical particle structure with chain-like aggregation attributed to van der Waals interactions. The presence of active components, K_2CO_3 and K_2O, confirms its classification as a typical supported solid alkali catalyst with excellent physicochemical stability.

(2) Systematic single-factor optimization experiments identified the optimal conditions for biodiesel synthesis as follows: a catalyst dosage of 6 wt% (relative to the mass of raw oil), an alcohol-to-oil molar ratio of 14:1, a reaction temperature of 60 °C, and a reaction time of 3 h. Under these conditions, a high biodiesel yield of 95.29% was obtained, underscoring the superior catalytic efficiency of the K_2CO_3/BCN catalyst in the transesterification process.

(3) An RSM optimization model was constructed using a four-factor, three-level BBD, accompanied by a quadratic polynomial regression equation established based on 29 experimental runs, systematically revealing the interaction effects among reaction temperature, reaction time, alcohol-to-oil molar ratio, and catalyst dosage. The optimized conditions identified by the model—temperature of 61.1 °C, reaction time of 3.3 h, alcohol-to-oil molar ratio of 14.2:1, and catalyst dosage of 6.1%—yielded a biodiesel conversion rate of 95.37% in validation experiments, confirming the model's reliability and applicability for process optimization.

Author Contributions: Conceptualization, C.L.; data curation, C.L. and T.S.; formal analysis, C.L., Y.C. and L.Z.; funding acquisition, Y.C. and X.X.; investigation, Y.C., Z.Y. and L.X.; methodology, C.L. and Y.L.; writing—original draft, T.S. and C.L.; writing—review and editing, Y.L. and X.X. All authors have read and agreed to the published version of the manuscript.

Funding: This work was funded by Excellent Research and Innovation Teams Project of Anhui Province's Universities (2022AH010092), Horizontal Research Project of Chaohu University (hxkt20250002), Anhui Province University Science and Engineering Teachers' Internship Program in Enterprises (2024jsqygz89), Discipline Construction Quality Improvement Project of Chaohu University (XLZ202307), Scientific Research Planning Project of Anhui Provincial (2022AH051726), National College Students' Innovation and Entrepreneurship Training Program of China (202510380028) and Anhui Province Postdoctoral Research Project (2024A773).

Data Availability Statement: The original contributions presented in the study are included in the article; further inquiries can be directed to the corresponding author.

Conflicts of Interest: Authors Chuan Li, Yijun Chen and Li Zhang were employed by the company Huangshan Shangyi Rubber and Plastic Products Co., Ltd., author Lin Xu was employed by the company Pingxiang Best Insulator Group Co., Ltd. The remaining authors declare that the research was conducted in the absence of any commercial or financial relationships that could be construed as a potential conflict of interest.

References

1. Mishra, V.K.; Goswami, R. A review of production, properties and advantages of biodiesel. *Biofuels* **2017**, *9*, 273–289. [CrossRef]
2. Betha, R.; Balasubramanian, R. Particulate emissions from a stationary engine fueled with ultra-low-sulfur diesel and waste-cooking-oil-derived biodiesel. *J. Air Waste Manag. Assoc.* **2011**, *61*, 1063–1069. [CrossRef]
3. Wu, Y.; Li, F.; Wang, W.; Ni, Z.; Ding, B.; Zhang, H. Experimental study on lubrication performance of main components of biodiesel. *Energy Sources Part A Recovery Util. Environ. Eff.* **2022**, *47*, 1–15. [CrossRef]
4. Suhara, A.; Karyadi; Herawan, S.G.; Tirta, A.; Idris, M.; Roslan, M.F.; Putra, N.R.; Hananto, A.L.; Veza, I. Biodiesel sustainability: Review of progress and challenges of biodiesel as sustainable biofuel. *Clean Technol.* **2024**, *6*, 886–906. [CrossRef]
5. Pydimalla, M.; Husaini, S.; Kadire, A.; Kumar Verma, R. Sustainable biodiesel: A comprehensive review on feedstock, production methods, applications, challenges and opportunities. *Mater. Today Proc.* **2023**, *92*, 458–464. [CrossRef]

6. Idoine, N.E.; Raycraft, E.R.; Hobbs, S.F.; Everett, P.; Evans, E.J.; Mills, A.J.; Currie, D.; Horn, S.; Shaw, R.A.; MacKenzie, A.C. *World Mineral Production 2018–2022*; BGS Press: Nottingham, UK, 2024. Available online: https://nora.nerc.ac.uk/id/eprint/537241/1/World%20Mineral%20Production%202018%20to%202022.pdf (accessed on 30 September 2025).
7. European Union (EU). Directive 2009/28/EC of the European Parliament and of the Council of 23 April 2009 on the Promotion of the Use of Energy from Renewable Sources and Amending and Subsequently Repealing Directives 2001/77/EC and 2003/30/EC. Available online: https://eur-lex.europa.eu/eli/dir/2009/28/oj/eng (accessed on 31 July 2025).
8. Chanakaewsomboon, I.; Phoungthong, K.; Palamanit, A.; Seechamnanturakit, V.; Cheng, C.K. Biodiesel produced using potassium methoxide homogeneous alkaline catalyst: Effects of various factors on soap formation. *Biomass Convers. Biorefin.* **2021**, *13*, 9237–9247. [CrossRef]
9. Golmakani, M.T.; Niakousari, M.; Peykar, A.; Safaeipour, T. Microwave-assisted transesterification of sour cherry kernel oil for biodiesel production: Comparison with ultrasonic bath-, ultrasonic probe-, and ohmic-assisted transesterification methods. *Grasas Aceites* **2024**, *75*, e545. [CrossRef]
10. Olagunju, O.A.; Musonge, P.; Kiambi, S.L. Production and optimization of biodiesel in a membrane reactor, using a solid base catalyst. *Membranes* **2022**, *12*, 674. [CrossRef]
11. Cong, W.-J.; Wang, Y.-T.; Li, H.; Fang, Z.; Sun, J.; Liu, H.-T.; Liu, J.-T.; Tang, S.; Xu, L. Direct production of biodiesel from waste oils with a strong solid base from alkalized industrial clay ash. *Appl. Energy* **2020**, *264*, 114735. [CrossRef]
12. Raising Rathod, D.; Suresh Karkal, S.; Jamadar, A.S.; Hashem, A.M.A.; Suresh, P.V.; Mamatha, S.S.; Kudre, T.G. Prospects of novel heterogeneous base catalysts and nanocatalysts in achieving sustainable biodiesel production. *Int. J. Green Energy* **2023**, *21*, 1017–1042. [CrossRef]
13. Kingkam, W.; Maisomboon, J.; Khamenkit, K.; Nuchdang, S.; Nilgumhang, K.; Issarapanacheewin, S.; Rattanaphra, D. Preparation of CaO@CeO_2 solid base catalysts used for biodiesel production. *Catalysts* **2024**, *14*, 240. [CrossRef]
14. Singh, S.; Bairagi, P.K.; Verma, N. Candle soot-derived carbon nanoparticles: An inexpensive and efficient electrode for microbial fuel cells. *Electrochim. Acta* **2018**, *264*, 119–127. [CrossRef]
15. Xiang, C.; Liu, S.Y.; Fu, Y.; Chang, J. A quick method for producing biodiesel from soy sauce residue under supercritical carbon dioxide. *Renew. Energy* **2019**, *134*, 739–744. [CrossRef]
16. Baig, A.; Ng, F.T.T. A single-step solid acid-catalyzed process for the production of biodiesel from high free fatty acid feedstocks. *Energy Fuels* **2010**, *24*, 4712–4720. [CrossRef]
17. Chen, X.; Qian, W.-W.; Lu, X.-P.; Han, P.-F. Preparation of biodiesel catalysed by KF/CaO with ultrasound. *Nat. Prod. Res.* **2012**, *26*, 1249–1256. [CrossRef]
18. Weremfo, A.; Abassah-Oppong, S.; Adulley, F.; Dabie, K.; Seidu-Larry, S. Response surface methodology as a tool to optimize the extraction of bioactive compounds from plant sources. *J. Sci. Food Agric.* **2023**, *103*, 26–36. [CrossRef]
19. Breig, S.J.M.; Luti, K.J.K. Response surface methodology: A review on its applications and challenges in microbial cultures. *Mater. Today Proc.* **2021**, *42*, 2277–2284. [CrossRef]
20. Mäkelä, M. Experimental design and response surface methodology in energy applications: A tutorial review. *Energy Convers. Manag.* **2017**, *151*, 630–640. [CrossRef]
21. Abu-Ghazala, A.H.; Abdelhady, H.H.; Mazhar, A.A.; El-Deab, M.S. Exceptional room temperature catalytic transesterification of waste cooking oil to biodiesel using environmentally-benign K_2CO_3/γ-Al_2O_3 nano-catalyst. *Chem. Eng. J.* **2023**, *474*, 145784. [CrossRef]
22. Li, C.; Wei, D.; Zhuang, Y.; Song, R.; Hu, X. Effect of biodiesel soot on tribological behavior of liquid paraffin. *China Pet. Process. Petrochem. Technol.* **2018**, *20*, 106–113.
23. Deng, X.; Mammen, L.; Butt, H.J.; Vollmer, D. Candle soot as a template for a transparent robust super-amphiphobic coating. *Science* **2012**, *335*, 67–70. [CrossRef]
24. Li, C.; Hu, X.; Feng, W.; Wu, B.; Wu, K. A supported solid base catalyst synthesized from green biomass ash for biodiesel production. *Energy Sources Part A Recovery Util. Environ. Eff.* **2017**, *40*, 142–147. [CrossRef]
25. Zhang, B.; Hu, E.Z.; Liu, T.X.; Hu, X.G. Characterization of morphology, structure and composition of soot particles from biomass fuel. *CIESC J.* **2015**, *66*, 441–448. [CrossRef]
26. Sulaiman, N.F.; Wan Abu Bakar, W.A.; Ali, R. Response surface methodology for the optimum production of biodiesel over Cr/Ca/γ-Al_2O_3 catalyst: Catalytic performance and physicochemical studies. *Renew. Energy* **2017**, *113*, 697–705. [CrossRef]
27. Li, F.-J.; Li, H.-Q.; Wang, L.-G.; Cao, Y. Waste carbide slag as a solid base catalyst for effective synthesis of biodiesel via transesterification of soybean oil with methanol. *Fuel Process. Technol.* **2015**, *131*, 421–429. [CrossRef]
28. Ergan, B.T.; Yılmazer, G.; Bayramoğlu, M. Fast, High Quality and Low-Cost Biodiesel Production using Dolomite Catalyst in an Enhanced Microwave System with Simultaneous Cooling. *Clean. Chem. Eng.* **2022**, *3*, 100051. [CrossRef]
29. Oza, S.; Kodgire, P.; Kachhwaha, S.S. Analysis of RSM based BBD and CCD techniques applied for biodiesel production from waste cotton-seed cooking oil via ultrasound method. *Anal. Chem. Lett.* **2022**, *12*, 86–101. [CrossRef]

30. Roslan, N.A.; Zainal Abidin, S.; Abdullah, N.; Osazuwa, O.U.; Abdul Rasid, R.; Yunus, N.M. Esterification reaction of free fatty acid in used cooking oil using sulfonated hypercrosslinked exchange resin as catalyst. *Chem. Eng. Res. Des.* **2022**, *180*, 414–424. [CrossRef]
31. Kefale Mangesha, Y.; Nallamothu, R.B.; Ancha, V.R.; Tesfaye Tefera, N. Optimization, Production, and characterization of cottonseed methyl ester based on Box-Behnken in response surface design and gas Chromatography-Mass spectrum analysis. *Energy Convers. Manag. X* **2024**, *23*, 100619. [CrossRef]
32. Nirmala, N.; Dawn, S.S. Optimization of Chlorella variabilis. MK039712.1 lipid transesterification using Response Surface Methodology and analytical characterization of biodiesel. *Renew. Energy* **2021**, *179*, 1663–1673. [CrossRef]

Disclaimer/Publisher's Note: The statements, opinions and data contained in all publications are solely those of the individual author(s) and contributor(s) and not of MDPI and/or the editor(s). MDPI and/or the editor(s) disclaim responsibility for any injury to people or property resulting from any ideas, methods, instructions or products referred to in the content.